Chemical Papers (2022) 76:65–77
https://doi.org/10.1007/s11696-021-01835-0

ORIGINAL PAPER

Green synthesis of silver nanoparticles using *Diplazium esculentum* extract: catalytic reduction of methylene blue and antibacterial activities

Atieya Abdul Hadi[1] · Jia Ya Ng[2] · Mustaffa Shamsuddin[2] · Juan Matmin[2] · Nik Ahmad Nizam Nik Malek[1,3]

Received: 10 May 2021 / Accepted: 22 August 2021 / Published online: 29 August 2021

Abstract

A green approach for the biosynthesis of silver nanoparticles (AgNPs) was developed using *Diplazium esculentum* aqueous extract as green reductant. The bio-stabilized AgNPs were characterized by UV–visible spectroscopy (UV–Vis), Fourier transform infrared spectroscopy (FTIR), X-ray diffraction (XRD), dynamic light scattering (DLS), and high-resolution transmission electron microscopy (HRTEM). The formation of AgNPs was indicated by the colour change and the absorption peak at 449 nm in the UV–Vis spectrum. FTIR spectral analysis suggested the possible biomolecules associated with the reduction of silver ions. The crystalline and face-centered cubic (fcc) structure of AgNPs was obtained by the XRD study. HRTEM analysis showed that the biosynthesized AgNPs composed of quasi-spherical, hexagonal, and ellipsoidal shapes with an average particle size of 23.385 ± 8.349 nm. The biosynthesized AgNPs exhibited good catalytic activity up to 91% reduction of Methylene blue (MB), which followed a reductive pathway rather than a photocatalytic route. The catalytic reduction follows a pseudo-first-order reaction with a rate constant of 0.1051 min^{-1}. The disc diffusion technique (DDT) and minimal inhibitory concentration (MIC) results showed significant antibacterial capability against Gram-positive (*Escherichia coli* ATCC 11,229) and Gram-negative (*Staphylococcus aureus* ATCC 6538) bacteria.

Keywords Green synthesis · Silver nanoparticles · *Diplazium esculentum* · Methylene blue · Antibacterial activity

Introduction

Metal nanoparticles such as gold, silver, and platinum have gained great attention due to their significant roles in the fields of catalysis, electronics, biomedical, environmental, and pharmaceuticals (Khan et al. 2019). Among the metal nanoparticles, silver nanoparticles (AgNPs) have been widely used due to their high catalytic, antimicrobial, and anti-inflammatory properties (Ebrahiminezhad et al. 2016; Vijilvani et al. 2020; Albukhari et al, 2019). AgNPs are commonly synthesized using chemical and physical methods. However, these methods are expensive and require toxic and hazardous chemicals, which are harmful to the environment (Ijaz et al. 2020; Yacoob et al. 2020). This situation leads to a growing demand for developing eco-friendly synthesis to avoid the use of toxic and hazardous chemicals. In recent years, many types of biological materials are used in the biosynthesis of nanomaterials such as bacteria (Saeed et al. 2020), fungi (Feroze et al. 2020), algae (Aboelfetoh et al. 2017), and plants (Singh et al. 2016). Biosynthesis of metal nanoparticles using biological materials is simple, inexpensive, low energy, and non-toxic with high stability.

Green synthesis of AgNPs using plant extract becomes a better choice since the plant is safe for handling, cheap, and widely available, which is suitable for scalability purposes (Ahmed et al. 2016). The synthesis can be carried out at room temperature with a simple apparatus setup. It mainly requires these three components: (1) a metal precursor as a seed source such as silver nitrate, (2) a reducing agent to reduce Ag^{+} to Ag^{0}, and (3) a stabilizing agent to prevent agglomeration (Singh et al. 2016). The plant extract acts

✉ Mustaffa Shamsuddin
mustaffa@kimia.fs.utm.my

[1] Department of Biosciences, Faculty of Science, Universiti Teknologi Malaysia, Johor Bahru, 81310 Johor, Malaysia

[2] Department of Chemistry, Faculty of Science, Universiti Teknologi Malaysia, Johor Bahru, 81310 Johor, Malaysia

[3] Centre for Sustainable Nanomaterials, Ibnu Sina Institute for Scientific and Industrial Research, Universiti Teknologi Malaysia, Johor Bahru, 81310 Johor, Malaysia

as both reducing and stabilizing agents; thus, more reduction on the cost and usage of hazardous chemicals could be achieved. Plants contain a rich source of flavonoids, phenolic acids, and terpenoids that can be used for this synthesis (Latif et al. 2019). Several recent studies have reported the successful synthesis of AgNPs in the size range of 5–100 nm from plant extract. For example, spheroidal AgNPs with a size range of 5–20 nm were successfully synthesized using *Murraya koenigii* (Qais et al. 2019). Jain and Mehata (2017) used leaf extract of *Ocimum sanctum* to synthesize AgNPs with sizes between 10 and 20 nm. Zafar and Zafar (2019) reported the synthesis of spherical-shaped AgNPs with a diameter between 20 and 100 nm using aqueous extracts obtained from fruits of *Phoenix dactylifera.* Spherical crystalline AgNPs with an average particle size of 20 nm were successfully produced using *Cestrum nocturnum* extract (Keshari et al. 2020).

Diplazium esculentum (D. esculentum) is commonly known as 'pucuk paku' in Malaysia. It is an edible vegetable fern in the family of Athyriaceae that is commonly found in Malaysia, the Philippines, and India. The flavonoid compounds found in this plant are procyanidin, kaempferol 3–O–rutinoside, and quercetin 3–O–glucoside (Umi kalsom et al. 1994). The dominant flavonoid content is quercetin with 213 mg/kg dry weight (Mien and Mohamed 2001). Although there have been extensive studies on the biosynthesis of AgNPs, it is anticiptated that different type of plant extract and its concentration may influence the morphology of the AgNPs formed. To the best of our knowledge, there is no available report on the use of this edible plant extract in the synthesis of metal nanoparticles especially AgNPs.

Metal nanoparticles are promising agents for the catalytic reduction of organic dyes (Ismail et al. 2019; Kim et al. 2021). Organic dyes are coloured molecules that are highly resistant to biological degradation due to their synthetic origin and complex chemical structure. They are used in numerous industries such as food, pharmacy, cosmetics, paints, plastics, paper, and textiles (Ali et al. 2005). The release of dye effluents into water sources can lead to serious environmental problems. Various conventional treatments such as coagulation, filtration, adsorption, and reverse osmosis have been used for dye removal. However, it is difficult to eliminate these dyes from water owing to their aromatic structural stability (Prasad et al. 2018). Thus, the application of AgNPs could offer an efficient yet simple method for dyes removal due to their relatively large surface-to-volume ratios.

In addition, AgNPs have been broadly used as antibacterial and anticancer agents for biomedical applications in the healthcare industry as a potential substitute for antibiotics (Lee and Jun 2019). The application of antibiotics is the most common approach to treat an infection. However, the rise of resistant organisms has made routine antibiotic prophylaxis ineffective. Furthermore, the rapid formation of biofilm on the implant surface by bacterium causes the antibiotics unable to penetrate and develop the antibacterial function. Thus, bactericidal activity of AgNPs without toxicity to human cells gained great highlight as an antibacterial agent that can kill drug-resistant bacteria and prevent infections (Yun'an Qing et al. 2018).

The present study reports the synthesis of AgNPs with *D. esculentum* aqueous extract acting as the reducing and stabilizing agent. The performance of the green synthesized AgNPs was evaluated based on the catalytic reduction of methylene blue (MB) in the presence of sodium borohydride ($NaBH_4$). The antibacterial activities of the synthesized AgNPs against Gram-negative (*Escherichia coli*) and Gram-positive (*Staphylococcus aureus*) bacteria were also investigated.

Materials and methods

Materials

Silver nitrate ($AgNO_3$) with a purity of 99.9% was purchased from Sigma-Aldrich (Aldrich, Germany). Sodium borohydride ($NaBH_4$) and methylene blue were procured from Merck and Hudson (Merck, Germany), respectively. Fresh leaves of *D. esculentum* (pucuk paku) were obtained from a local market in Skudai, Johor, Malaysia.

Preparation of 2% w/v D. esculentum aqueous extract

The leaves of *D. esculentum* were cut into small pieces, washed thoroughly with deionized (DI) water to remove dust, and air-dried for several days. The air-dried *D. esculentum* leaves were then ground into powder using an electrical blender, sieved using an 850 mm sieve, and kept in an air-tight plastic container for further use.

The leaves powder (2.0 g) was mixed with 100 mL of DI water and boiled for 15 min with continuous stirring. After the solution was allowed to cool to room temperature, it was filtered using Whatman filter paper No. 1. The filtered extract was stored in a refrigerator at 5 ℃ until further use.

Synthesis of AgNPs by aqueous leaf extract of D. esculentum

In volumetric flasks (1, 2, 3, 4 and 5 mL), 1 mL of 2% (w/v) *D. esculentum* aqueous extract was added to 1 mM of 10 mL $AgNO_3$ solution at room temperature. The colour change from light yellow to light brown indicated the formation of the colloidal AgNPs. The formation of AgNPs was monitored using UV–Vis spectroscopy. The reaction time for the

formation of AgNPs was recorded until it reached saturation. The biosynthesized AgNPs were collected by centrifugation at 14,500 rpm for 15 min and washed with DI water twice to remove any excess plant extract on the surface of the AgNPs. The synthesis of AgNPs was optimized by varying the amount of leaf extract from 1 to 5 mL. The biosynthesized AgNPs obtained were stored in a vacuum dessicator prior to any characterization.

Characterization of the biosynthesized AgNPs

The colloidal AgNPs formation progress was monitored by UV–Vis spectroscopy using a Shimadzu 2501 PC UV–Vis spectrophotometer (Shimadzu, Kyoto, Japan). The UV–Vis spectra of the aqueous extract and $AgNO_3$ mixture were recorded at regular time intervals in a 1 cm path length quartz cuvette in the wavelength range from 200 to 800 nm. The functional groups of the phytochemicals responsible for the reduction and stabilization of the AgNPs were identified by FTIR spectroscopy. The infrared spectra were recorded using Perkin Elmer 1600 model Fourier Transform Infrared (FTIR) spectrometer (Perkin Elmer, Norwalk, CT, USA) in the spectral range of 4000 to 400 cm^{-1} using the potassium bromide (KBr) disc method. The crystalline nature of the biosynthesized AgNPs was characterized using a Bruker D8 Advance X-ray Diffractometer (XRD, Bruker, Germany) with CuKα radiation (λ = 1.5418 Å). The samples were measured in the range of 2θ = 10–100°. The diffraction patterns were indexed from the database files to determine the crystalline phases and structural properties of AgNPs.

In the dynamic light scattering (DLS) measurement, the hydrodynamic particle sizes were analysed using a Malvern Zetasizer Nano ZSP (Malvern Instruments, Malvern, UK) operating with a He–Ne laser at a wavelength of 633 nm. Using the DLS principle, the average particle size dispersed in a liquid medium was calculated with a scattering angle of 173°. The standard viscosity and refractive index values used for pure water (25 °C) were 0.8872 mPa and 1.33, respectively.

The shape, size, and morphology of the AgNPs were studied using a JEOL JEM-ARM 200F HR-TEM microscope (JEOL, Tokyo, Japan) operated at 200 kV. Samples for TEM analysis were prepared by placing a small drop of sonicated colloidal AgNPs solution on a carbon-coated copper grid. The excess solution from the TEM grid was removed, and the grid was allowed to dry under ambient conditions before the analysis.

The catalytic action of biosynthesized AgNPs on Methylene Blue

The catalytic activity of the prepared AgNPs was assessed in the removal of methylene blue (MB) by $NaBH_4$. In a typical assay, 10 mL of 10 ppm stock solution of MB was mixed with 3 mL of freshly prepared 5 mM $NaBH_4$ solution. 3 mg of the biosynthesized AgNPs was added into the previously prepared mixture of MB and $NaBH_4$. The mixture was continuously stirred at room temperature, and the reduction of MB was monitored at a regular interval of 5 min by UV–Vis spectrophotometer. The value of absorption band maxima was recorded. A control experiment was also prepared in the absence of AgNPs.

Antibacterial activity assay of biosynthesized AgNPs

The antibacterial activity of the biosynthesized AgNPs was assessed against Gram-positive bacteria *S. aureus* (ATCC 6538) and Gram-negative bacteria *E. coli* (ATCC 11,229). Agar disc diffusion technique (DDT) and minimum inhibitory concentration (MIC) were used to evaluate the antibacterial properties of biosynthesized AgNPs based on the Clinical Laboratory Standard Institute guidelines (CLSI, 2018). Procedures were done strictly under the aseptic condition to avoid contamination (Bykowski and Stevenson, 2020). Both assays used distilled water as a negative control and Kanamycin as a positive control.

The DDT procedure was performed according to the published protocol by Aminullah et al., (2021) with some modifications. The turbidity of the bacterial cell was adjusted to a scale of 0.5 using MacFarland standard with approximately 10^8 CFU (Colony Forming Unit)/mL cells concentration (CLSI, 2018). Bacterial suspensions were then spread onto Mueller–Hinton Agar (MHA) plates using sterile cotton swabs. The sterile disc (6 mm diameter) was saturated with 100 µL of colloidal AgNPs at varying concentrations (50 µg, 100 µg, and 150 µg) before being placed carefully on the inoculated agar. After 24 h of incubation at 37 °C, the diameter of the growth inhibition zones around the disc was measured and recorded as mean diameter ± SD.

Minimal inhibitory concentration (MIC) was evaluated using the dropped plate technique (Naghili et al. 2013). About 50 mL of the bacterial cells in a log phase (optical density of 0.6 to 0.8 measured at 600 nm) was centrifuged at 4000 rpm at 4 ºC for 15 min (Mytilinaios et al., 2012). The bacterial pellets were washed twice and suspended in 200 mL of saline solution (9.0% of NaCl). Then, 10 mL of the bacterial suspension was added to the different AgNPs concentrations between 20 to 140 µL/mL. The mixture was shaken at 100 rpm for 30 min. Finally, 10 µL from

the sample solution was pipetted accurately and dropped on the surface of the MHA plate, and incubated at 37 °C overnight. The plate was observed for the growth of the bacteria.

Results and discussion

Biosynthesis of AgNPs

Biosynthesis of AgNPs was performed using an aqueous extract of *D. esculentum* as the reducing and capping agent. The biomolecules present in the extract play an essential role in stabilizing the AgNPs from agglomeration. To obtain an optimum value of colloidal AgNPs, different amounts of the extract (1–5 mL) were added to a constant concentration of $AgNO_3$ solution (1 mM), which acted as the metal precursor. The formation of the colloidal AgNPs was initially confirmed by the colour change of the solution. The reduction process from Ag(I) to the elemental Ag was observed based on the colour changed in the mixture of $AgNO_3$ and *D. esculentum* aqueous extract solution from pale yellow to deep brown, as shown in Fig. 1. The deep brown colour of the reaction mixture was developed due to the excitation of the Surface Plasmon Resonance (SPR) vibrations in AgNPs (Rajeshkumar S. 2016). The formation of colloidal AgNPs was monitored using UV–Vis spectroscopy.

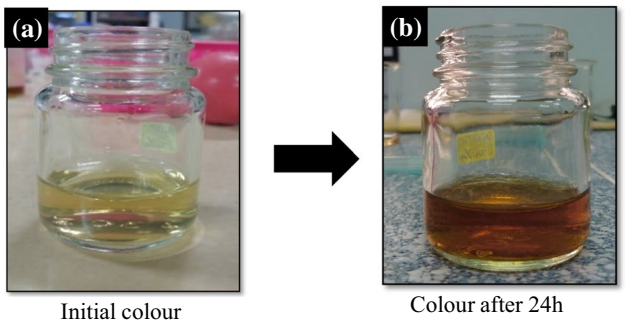

Fig. 1 Colour changes in the reaction mixture of $AgNO_3$ and *D. esculentum* **a** before and **b** after 24 h

In Fig. 2a, the UV–Vis spectra show the absorbance of $AgNO_3$-*D. esculentum* mixtures at different volumes of added *D. esculentum* extract. The SPR band of AgNPs centred around 450 ± 5.0 nm had increased in the absorption when the volume of the *D. esculentum* extract added increased from 1 to 2 mL, suggesting a higher yield of AgNPs produced. At a higher amount of *D. esculentum* extract (3 to 5 mL), the SPR bands exhibited broader absorption with lower absorbance, probably due to the aggregation of AgNPs (Lade and Gogle 2019). Likely, the presence of too many reducing agents might contribute to the secondary reduction process on the surface of the nuclei, thus forming larger particles of AgNPs entities (Borhamdin et al. 2016). Therefore, 2 mL of *D. esculentum* extract aqueous was found to be the optimum volume for the biosynthesis of AgNPs as it gave the highest yield of colloidal AgNPs.

Figure 2b indicates the SPR band of AgNPs as a function of reaction time, in which the absorption intensity was gradually increased with time. Figure 2c corresponds to the plot absorbance at l = 449 nm against the time of reaction, in which the reduction was almost complete within 24 h. Thus, the AgNPs can be synthesized within 24 h using this green method by employing the *D. esculentum* aqueous extract as the reducing agent. On continuous monitoring, the absorbance of the colloidal AgNPs was almost constant for more than 48 h. This finding suggested that the AgNPs were stable and did not undergo agglomeration in 48 h. Hence, *D.*

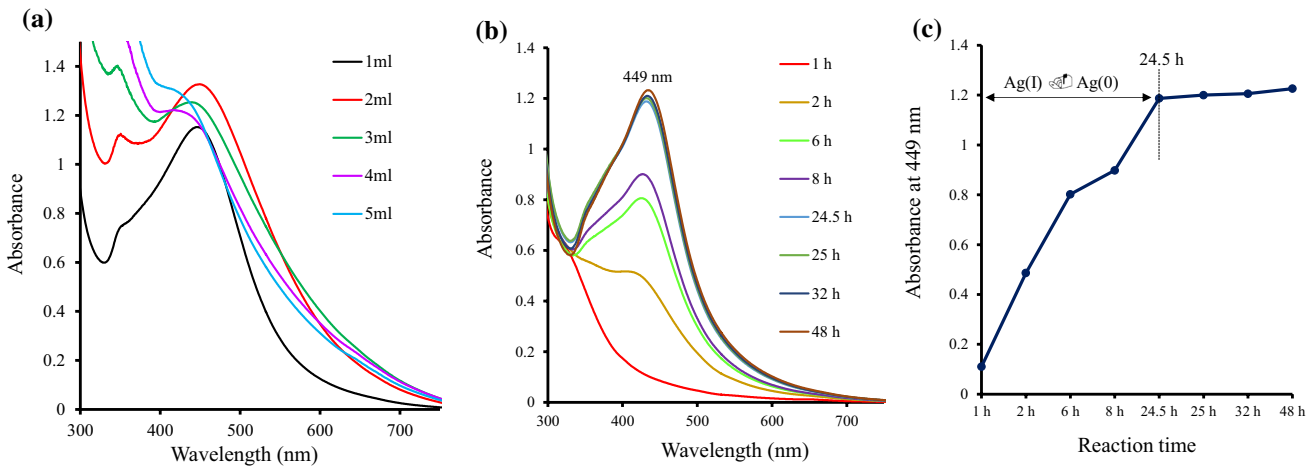

Fig. 2 **a** UV–Vis spectra of colloidal AgNPs synthesized using different volumes of *D. esculentum* aqueous extract, **b** UV–Vis spectra for the formation of AgNPs against time, and **c** Plot of absorbance at λ = 449 nm versus time

esculentum aqueous extract contained biomolecules that effectively stabilized the surface of AgNPs and prevented it from further growth and agglomeration.

The FTIR spectra were recorded to identify the functional groups of the biomolecules present in the *D. esculentum* extract, which are responsible for the surface stabilization of biosynthesized AgNPs (Fig. 3). The FTIR spectrum of the *D. esculentum* powder displayed a broad absorption band at 3393 cm^{-1} assigned to O–H groups stretching vibrations of phenols and alcohols (Ahmed et al. 2016). Meanwhile, weak bands around 2900 cm^{-1} were due to C-H asymmetric stretching represented alkanes in lipids (Paul et al. 2015). Absorption bands observed at 1645 and 1065 cm^{-1} were consistent with the presence of C = O and C–O stretching vibrations, respectively (Jain and Mehata 2017).

Based on a previous report, these functional groups in the *D. esculentum* powder were indicated as flavonoid compounds such as procyanidin, kaempferol 3–O–rutinoside, and quercetin 3–O–glucoside (Paul et al. 2015). Meanwhile, the FTIR spectrum of the biosynthesized AgNPs showed similar absorption bands of OH, C = O, and C–O with less intensity and a small shift in the position, as shown in Table 1. The presence of these similar bands strongly suggested that the surface of the nanoparticles was capped with phytomolecules such as flavonoids, polyphenols, with functional groups such as ketone, aldehyde carboxylic acid, and others (Chand et al. 2020). These surface adsorbed biomolecules prevented the aggregation of AgNPs. Thus, the *D. esculentum* extract contained compounds with OH and CO groups, which have vital roles in reducing and stabilizing AgNPs.

XRD diffractogram of the biosynthesized AgNPs was depicted in Fig. 4. The obtained diffractogram confirmed the crystalline structure of biosynthesized AgNPs. The XRD pattern revealed five distinct diffraction peaks at 37.93˚, 44.23˚, 64.34˚, 77.27˚, and 81.29˚corresponded to the lattice planes (111), (200), (220), (311), and (222), respectively. The peak positions and diffraction lines intensities matched well with the standard reference of silver (ICDD no. 03–065–2781) in the face-centred cubic (fcc) structure. The d-spacing of AgNPs measured using Bragg's Law (2.37 Å) showed a good agreement with the literature value (Bhakya et al. 2015). The appearance of a broad amorphous peak between 0 to 30° indicated the existence of biomolecules from the *D. esculentum* presented on the surface of AgNPs. The average crystallite size of AgNPs (19.9 nm) was calculated using Debye–Scherrer determined from the width of the (111) plane.

Table 1 FTIR peak assignment for *D. esculentum* and biosynthesized AgNPs

Functional group	Wavenumber (cm^{-1})	
	D. Esculentum leaves	Biosynthesized AgNPs
O–H	3393	3398
C–H	2928, 2851	2912, 2848
C = O	1645	1621
C–O	1065	1048

The size, dispersion, and morphology of the biosynthesized AgNPs were examined using HRTEM image analysis. The HRTEM images at different magnifications are shown in Fig. 5a–d. As illustrated, the AgNPs have mostly quasi-spherical, with some in hexagonal and ellipsoidal shape. The lattice fringes of 0.2378 nm were measured using Gatan software, which corresponded to the lattice plane of (111) and was consistent with the literature value (Ren et al. 2016). Meanwhile, Fig. 5e shows the particle size distribution histogram of the biosynthesized AgNPs generated using the Image-*J* software. The particle size distribution was in the range of 6–47 nm, with an average particle size of 23.385 ± 8.349 nm.

The DLS particle size distribution profile of the biosynthesized AgNPs is shown in Fig. 6. The particle size of AgNPs was measured in terms of hydrodynamic diameter

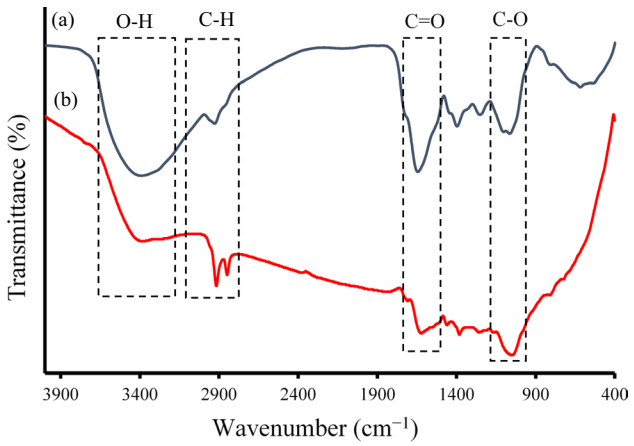

Fig. 3 FTIR spectra of **a** *D. esculentum* leaves powder **b** AgNPs

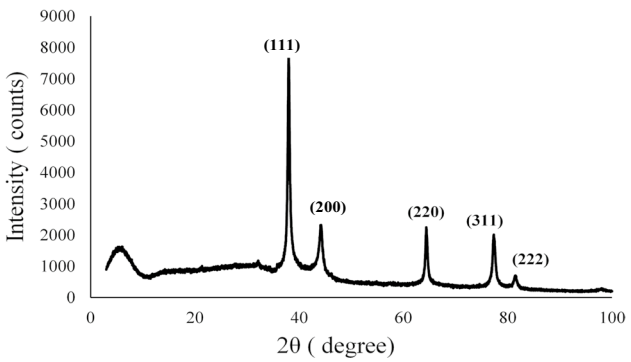

Fig. 4 XRD diffraction pattern of AgNPs

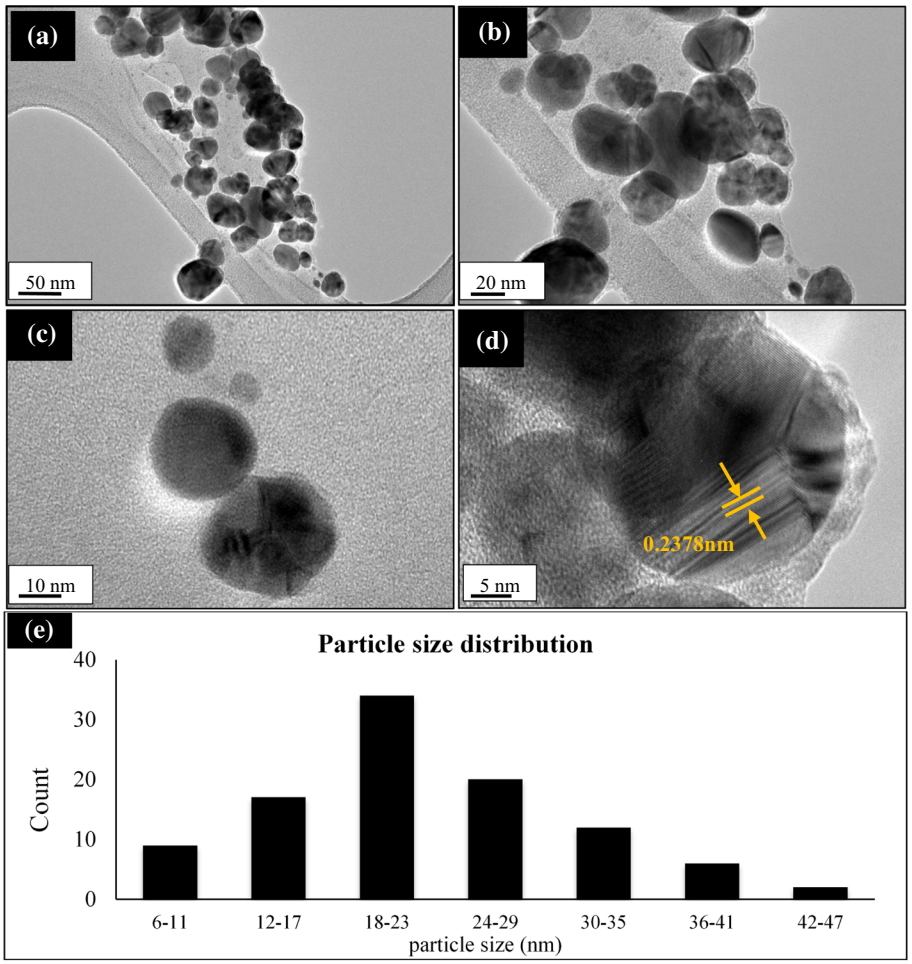

Fig. 5 **a**-**c** HRTEM images of AgNPs at different magnifications, **d** Lattice fringes spacing and **e** Particle size distribution histogram

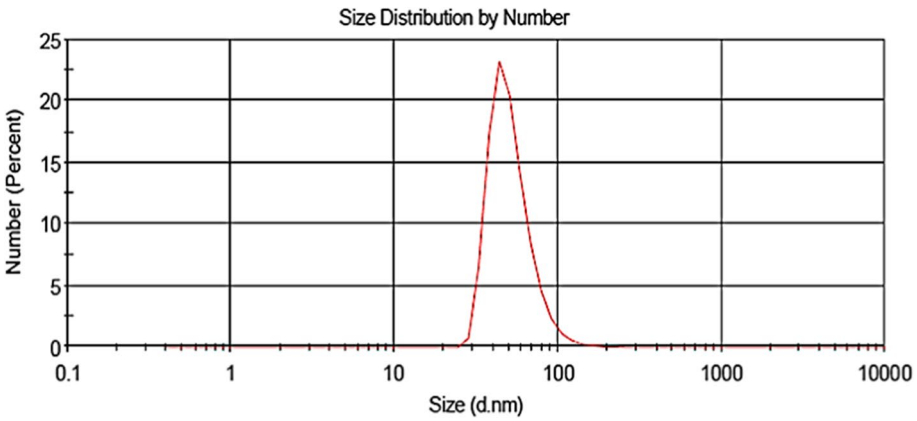

Fig. 6 Particle size distribution of AgNPs solution by DLS

in the colloidal suspension (Baranwal et al. 2016). Based on the result, the calculated average particle size of the biosynthesized AgNPs was 52.06 nm. As expected, the particle size measured using DLS in solution was larger than the crystallite size obtained from powder XRD and the particle size calculated from HRTEM analysis. The larger size obtained from DLS analysis was due to the layer of surface adsorbed biomolecules and solvent molecules on AgNPs (Sanyasi et al. 2016).

Catalytic reduction of aqueous methylene blue

AgNPs catalysed reduction of dyes has been well documented (Marimuthu et al. 2020). The catalytic performance

of the biosynthesized AgNPs was tested in the reduction reaction of methylene blue (MB) by $NaBH_4$ in an aqueous solution as a model reaction. The performance was monitored using UV–Vis spectrophotometry and visual inspection of the colour change of MB (Fig. 7). The initial dark blue aqueous MB solution typically showed a maximum absorption band at $\lambda = 664$ nm owing to the $n \rightarrow \pi^*$ transition (Saad et al. 2016). The catalytic reduction progress of MB was monitored based on the gradual decrease in the intensity of the absorption band at 664 nm until a colourless solution was obtained.

Figure 7a shows that the reduction rate of MB was significantly slower in the absence of AgNPs catalyst, in which 39% of reduction in 90 min was observed. In the presence of 3 mg of AgNPs, the reduction rate of MB increased to 91% of reduction in 90 min (Fig. 7b). These findings suggested the effective reduction of MB could be achieved in the presence of AgNPs at its optimal concentration. AgNPs were hypothesized as the active sites, acting as a mediator for the electron transfer step during the reduction of MB by $NaBH_4$ when the biosynthesized was used for the catalysed reduction. Recently, AgNPs were reported as good, highly efficient, and stable photocatalysts under ambient temperature with visible light illumination for degrading organic compounds and dyes (Wang et al. 2009; Kumari et al. 2016; Therumagal and Jeyakumari, 2020).

The catalytic removal of aqueous MB was also conducted under the dark condition to ascertain the photocatalytic removal pathway of MB. Figure 7c shows the decolourization percentage of MB performed under dark condition (91%) was similar to the value obtained by the catalytic reduction conducted under normal laboratory fluorescent lightings. The comparison is clearly shown in Fig. 7d. Hence, it could be deduced that the catalytic removal of MB by AgNPs followed the reductive pathway rather than the photocatalytic route. Similar previous findings have been reported on the catalytic reduction of MB in an aqueous solution by AgNPs in the presence of $NaBH_4$ as a reducing agent (Raza et al. 2016). The rate constant (k) was calculated from the plot of $\ln\left(A_t/A_0\right)$ against time as shown in Fig. 7e.

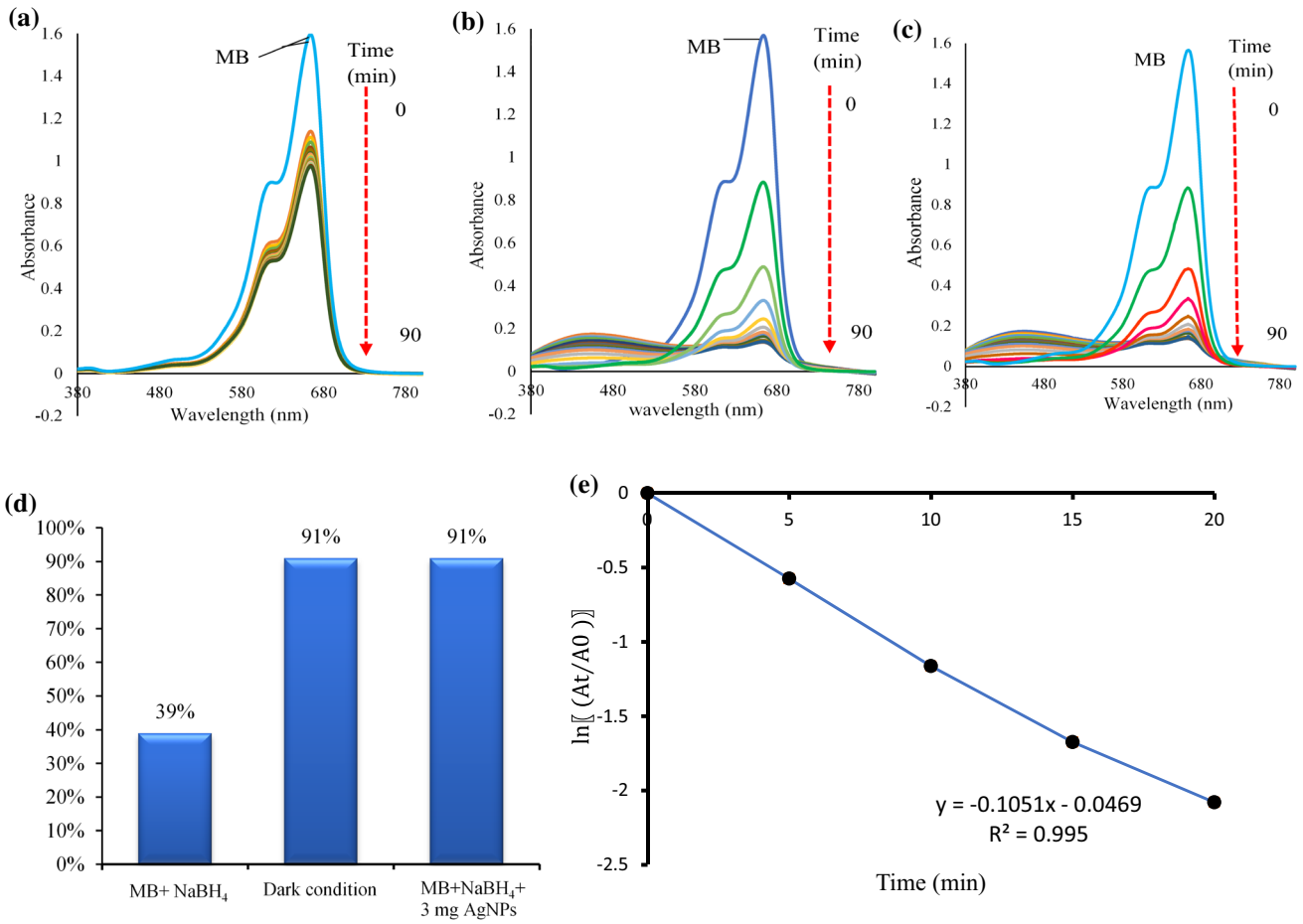

Fig. 7 UV–Vis spectra of reduction on **a** MB + $NaBH_4$, **b** MB + $NaBH_4$ + 3 mg AgNPs, **c** reduction reaction under dark condition, and **d** percentage of decolourization of aqueous MB, **e** Graph of ln(*At A*0) against time

The result shows that the reduction reaction of MB follows a pseudo-first-order kinetic with an average rate constant (k) value of 0.1051 min^{-1}. Thus, it can be concluded that the biosynthesized AgNPs can act as an effective catalyst for the degradation of organic dyes in waste water.

In the presence of AgNPs as the catalysts and $NaBH_4$ as a reducing agent, the rapid decolourization of MB could be due to the fast electron transfer between $NaBH_4$ and MB (Fig. 8). Specifically, $NaBH_4$ acts as an electron donor and MB as the electron acceptor. The catalytic progression follows a redox mechanism, in which the AgNPs mediates the transfer of electrons from donor BH_4^- ions to MB, which is the acceptor. This type of electron transfer phenomenon in which metal nanoparticles act as redox catalysts is known as the "electron relay effect" and has been similarly reported in the catalysed reduction of other dyes (Gupta et al. 2011).

Antibacterial assay

The antibacterial assay of the AgNPs was conducted against *Escherichia coli* (*E. coli*) and *Staphylococcus aureus* (*S. aureus*) through the disc diffusion technique (DDT) and minimum inhibition concentration (MIC). There was no formation of an inhibition zone for bacteria treated with *D. esculentum* leaf extract due to the absence of any antibacterial property, as shown in Fig. 9c. When respective bacteria were treated with increased concentrations of AgNPs, the sizes of the inhibition zone also increased, as shown in Fig. 9A, B. The inhibition zone values in Table 2 indicated that the AgNPs were more susceptible to *E. coli* compared to *S. aureus*. This susceptibility difference between these Gram-negative bacteria is most likely due to their structural variations, especially in their cell envelope (Jiraroj et al. 2014; Salim and Malek 2016). As Gram-negative bacteria lack the thick outer peptidoglycan layer presented in Gram-positive bacteria, *E. coli* is most likely to be inhibited first due to AgNPs anchorage and penetration to the cell wall (Mathur et al. 2018). Even though AgNPs are well known to possess antimicrobial properties, the mechanisms regarding their microbial toxicity are not clearly understand and reported.

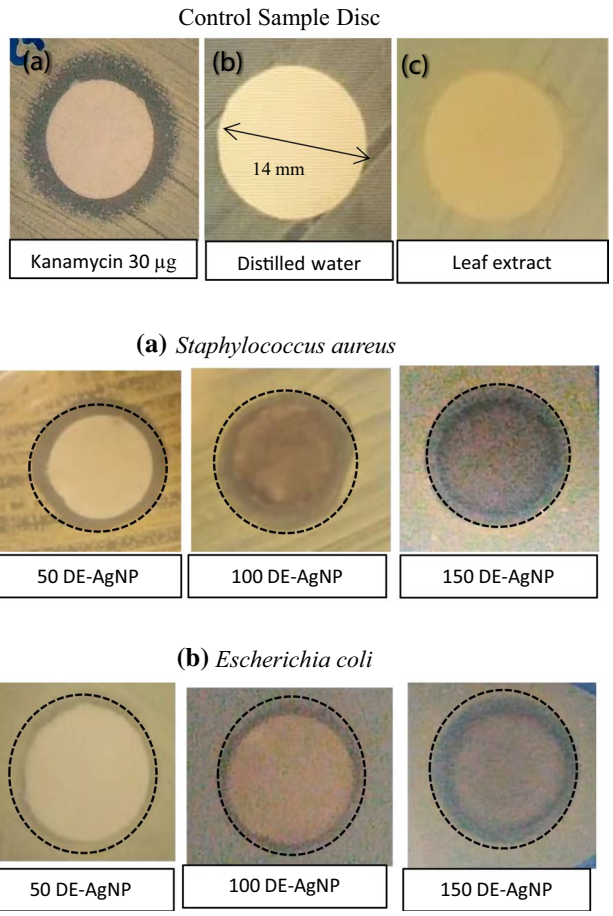

Fig. 9 Antibacterial activity of AgNPs against **A** *Staphylococcus aureus* **B** *Escherichia coli* at different concentrations (50–150 µg/mL). **a** positive control disc using Kanamycin 30 µg, **b–c** negative control using distilled water and leaf extract

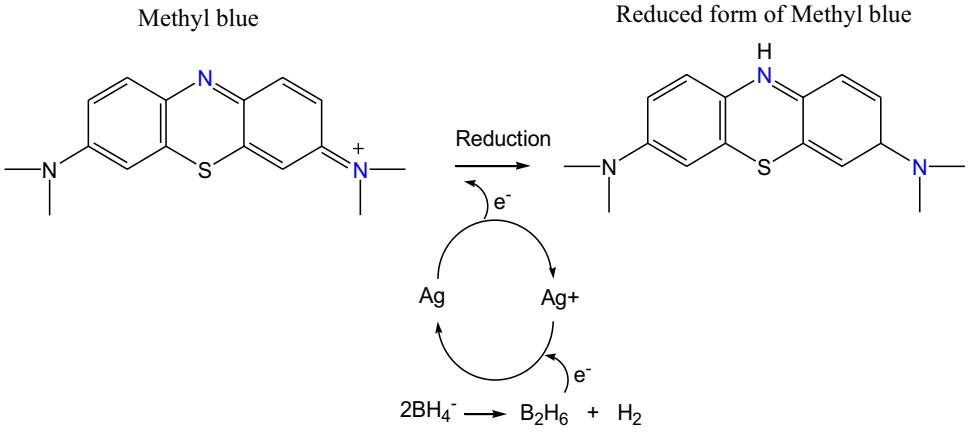

Fig. 8 Proposed mechanism for AgNPs catalysed reduction of MB by $NaBH_4$

Table 2 Inhibition zone diameter of the samples against Gram-positive bacteria *(S. aureus)* and Gram-negative bacteria *(E. coli)*

Sample (µg)	Mean diameter Zone of Inhibition ± SD	
	S. aureus	*E coli*
Distilled water	0	0
Leaf extract	0	0
Kanamycin (30)	17.5 ± 0.1	18 ± 0.0
AgNPs (50)	15.3 ± 0.2	16.7 ± 0.3
AgNPs (100)	16.9 ± 0.1	17.5 ± 0.2
AgNPs (150)	17.6 ± 0.2	17.8 ± 0.1

Diameter of disc = 14 mm. Kanamycin as a positive control, distilled water as a negative control

Table 3 Minimum inhibition concentration of biosynthesized AgNP towards *S. aureus* and *E. coli*; Kanamycin used as positive control

Bacterial strain	MIC value (µg/mL)	
	AgNPs	Kanamycin (control)
S. aureus	100	10
E. coli	100	5

Table 3 shows the MIC value for the biosynthesized AgNPs and Kanamycin as a positive control. The MIC value for biosynthesized AgNPs from *D. esculentum* toward both bacteria was 100 µg/mL. This value was in agreement with the MIC values obtained from chemically synthesized AgNPs of 30 nm in size by Agnihotri et al. (2014). Therefore, this study confirmed that the biosynthesized AgNPs exhibited good antibacterial properties comparable to the chemically synthesized silver nanoparticle with broad-spectrum activity.

The antibacterial properties projected by the DDT and MIC results are strongly correlated with the size, shape, surface charge, chemical composition and aggregation of the nanoparticles. Due to their strong intermolecular interaction, AgNPs are prone to aggregation, which reduces their antibacterial efficacy (Garcia et. al., 2020). Thus, for the significant antibacterial potency, it is critical to prevent AgNPs from aggregating and maintain their dispersion (Slavin et. al., 2017). In this study, the phytochemical compounds from *D. esculentum* acted as the capping agent to inhibit the aggregation of the AgNPs during synthesis.

Figure 10 depicts the antibacterial mechanism of AgNPs against bacterial cells. The capacity of AgNPs to kill bacteria is due to the release of silver ions from their surface, which can destroy molecules containing sulphur and

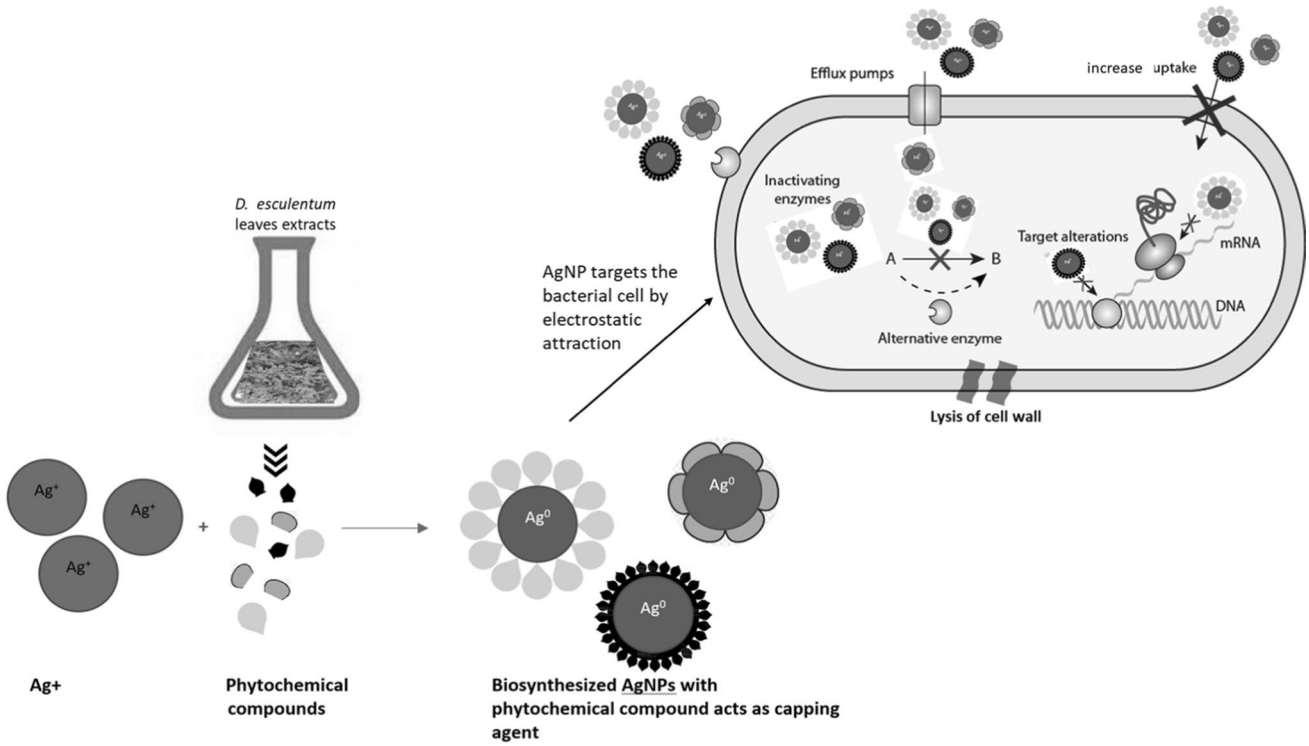

Fig. 10 Proposed antibacterial mechanisms for AgNPs towards bacteria

Table 4 Antibacterial and dye removal applications of AgNPs biosynthesized from plant extract

Plant extract	Country	Degradation of dye	Bioactivity	References
Diplazium esculentum	Malaysia	Methylene Blue	Antibacterial	This work
Caulerpa serrulate	Egypt	Congo red	Antibacterial	Aboelfetoh et al. 2017
Mesua Ferrea	India	Congo red	Antimicrobial	Thirumagal et al. 2020
Solanum nigrum	India	4-Nitrophenol	Antimicrobial	Vijilvani et al. 2020
Papaya	India	Blue CP, yellow 3RS	Antibacterial	Jain et al. 2020
Albizia procera	Pakistan	Methylene Blue	Antibacterial	Rafique et al. 2019
Ficus retusa	India	Eriochrome blact T dye	Antibacterial	Singhal et al. 2017
Aspilia pluriseta	Kenya	Congo red	Antimicrobial	Nyabola et al. 2020
Mentha aquatica	Iran	Methylene blue, Congo red, Rhodamin B, methyl orange	Antibacterial	Nouri et al. 2020

phosphorus, such as bacteria's DNA and proteins (Behravan et. al., 2019). The mode of action of AgNPs is generally described by simultaneous metal ion release, oxidative stress and non-oxidative mechanisms (Shaikh et al., 2019). Moreover, the generation of reactive oxygen species (ROS) inhibits the antioxidant defence system and causes mechanical damage to the cell membrane.

Unlike Ag^+ ions, AgNPs provide better contact with bacteria due to a larger surface area. AgNPs can directly interact with the proteins and phospholipids of the cell membrane by neutralization of the surface electric charge, violating its integrity and permeability (de Souza et al., 2019). Once within the cell, the AgNPs' bind to the thiol group (–SH) of respiratory enzyme active sites as well as subcellular organelles like mitochondria, causing the cell's homeostasis to be disrupted (Sooklert et al. 2019).

The AgNPs may also enter the nucleus through the cytoplasmic channels which finally lead to the fragmentation of the DNA double helix, thus disrupt their functions and inevitably lead to the cell's death (Dutta et al. 2020). In fact, one of the important mechanisms of AgNPs killing effect to bacteria is by increasing the production of internal ROS. This is because more reactive singlet oxygen metabolites (OH^-, O_2^-, H_2O_2) are abundantly generated in the presence of trace metal ions (Agarwal et al. 2019). Thus, at high concentrations of ROS, further damage to biomolecules occurs, in which AgNPs exhibit concentration-dependent antimicrobial activity against *E. coli* and *S. aureus*. These multiple mechanisms greatly endorse the advantage of the plant biosynthesized AgNPs to inhibit bacterial growth, thus killing it.

AgNPs have gained in popularity as a result of their improved ability to kill bacterial infections at lower concentrations than bulk silver (Ijaz et al. 2020). They are anticipated to be used in a wide range of applications, including cosmetics, biomedical devices, paints, textiles and even drinking water treatment membranes due to their diverse characteristics and physicochemical properties. Recent studies regarding dye degradation and antibacterial applications are listed in Table 4. As summarised in Table 4, there is no report yet employing this plant from Malaysia. The combination of catalytic and antibacterial properties exhibited by the AgNPs derived from the *D. esculentum* extract reported in this work is comparable with other plant-mediated syntheses AgNPs.

Conclusion

An environmentally benign and green synthesis of AgNPs had been successfully developed through the reduction of aqueous $AgNO_3$ using *D. esculentum* aqueous extract as reducing and stabilizing agent. . . UV–Vis spectral analytical data showed an absorption peak near 450 nm which demonstrates the successful formation of AgNPs. The presence of similar functional groups of *D. esculentum* in the FTIR spectrum of AgNPs indicated the function of *D. esculentum* as a reductant and stabilizer. HRTEM showed that biosynthesized AgNPs are mostly quasi-spherical with an average particle size of 23.385 ± 8.349 nm. The biosynthesized AgNPs were successfully proven as catalytically active in the reduction of aqueous methylene blue in the presence of sodium borohydride with 91% reduction. The antibacterial assay shows that biosynthesized AgNPs potentiates excellent antibacterial activity towards a broad spectrum of bacteria with a dose-dependent effect.

Funding The authors gratefully acknowledged the financial support from the Ministry of Higher Education (MOHE) Malaysia and Universiti Teknologi Malaysia (UTM) under the Trans-Disciplinary Research Program UTM-TDR 17.2(T1): Biomediated Shape and Size Control Synthesis of Silver Nanoparticles (AgNPs) using Malaysian Herbal Plant Extract (Vote 05G57). AA. Hadi thanked the Public Services Department, Malaysia, for a scholarship received through the Excellent Student Program.

Declarations

Conflict of interest The authors declare that they have no conflict of interest.

References

Aboelfetoh EF, El-Shenody RA, Ghobara MM (2017) Eco-friendly synthesis of silver nanoparticles using green algae (Caulerpa serrulata): reaction optimization, catalytic and antibacterial activities. Environ Monit Assess 189(7):1–15. https://doi.org/10.1007/s10661-017-6033-0

Agarwal H, Nakara A, Shanmugam VK (2019) Anti-inflammatory mechanism of various metal and metal oxide nanoparticles synthesized using plant extracts: A review. Biomed Pharmacother 109:2561–2572. https://doi.org/10.1016/j.biopha.2018.11.116

Agnihotri S, Mukherji S, Mukherji S (2014) Size-controlled silver nanoparticles synthesized over the range 5–100 nm using the same protocol and their antibacterial efficacy. RSC Adv 4(8):3974–3983. https://doi.org/10.1039/C3RA44507K

Ahmed S, Saifullah A, Ahmad M, Swami BL, Ikram S (2016) Green synthesis of silver nanoparticles using Azadirachta indica aqueous leaf extract. J Radiat Res Appl Sci 9:1–7

Ahmed S, Ahmad M, Swami BL, Ikram S (2016) A review on plants extract mediated synthesis of silver nanoparticles for antimicrobial applications: a green expertise. J Adv Res 7(1):17–28. https://doi.org/10.1016/j.jare.2015.02.007

Albukhari SM, Ismail M, Akhtar K, Danish EY (2019) Catalytic reduction of nitrophenols and dyes using silver nanoparticles@ cellulose polymer paper for the resolution of waste water treatment challenges. Colloids Surf A Physicochem Eng Asp 577:548–561. https://doi.org/10.1016/j.colsurfa.2019.05.058

Ali MF, El Ali BM, Speight JG. (2005) Handbook of industrial chemistry: organic chemicals. McGraw-Hill Education.

Aminullah F, Malek NA, Jemon K. (2021). Antibacterial activity of silver nanoparticles synthesized from Persicaria odorata (L.) sojak leaves extract. In AIP Conference Proceedings May 25. 2353(1), p. 030022. AIP Publishing LLC. https://doi.org/10.1063/5.0052607

Baranwal A, Mahato K, Srivastava A, Maurya PK, Chandra P (2016) Phytofabricated metallic nanoparticles and their clinical applications. RSC Adv 6(107):105996–106010

Behravan M, Panahi AH, Naghizadeh A, Ziaee M, Mahdavi R, Mirzapour A (2019) Facile green synthesis of silver nanoparticles using Berberis vulgaris leaf and root aqueous extract and its antibacterial activity. Int J Biol Macromol 124:148–154. https://doi.org/10.1016/j.ijbiomac.2018.11.101

Bhakya S, Muthukrishnan S, Sukumaran M, Muthukumar M, Kumar ST, Rao MV (2015) Catalytic degradation of organic dyes using synthesized silver nanoparticles: a green approach. J Bioremediat Biodegrad 6(5):1. https://doi.org/10.4172/2155-6199.1000312

Borhamdin S, Shamsuddin M, Alizadeh A (2016) Biostabilised icosahedral gold nanoparticles: synthesis, cyclic voltammetric studies and catalytic activity towards 4-nitrophenol reduction. J Exp Nanosci 11(7):518–530. https://doi.org/10.1080/17458080.2015.1090021

Bykowski T, Stevenson B (2020) Aseptic Tech Curr Protoc Microbiol 56(1):e98

Chand K, Cao D, Fouad DE, Shah AH, Dayo AQ, Zhu K, Lakhan MN, Mehdi G, Dong S (2020) Green synthesis, characterization and photocatalytic application of silver nanoparticles synthesized by various plant extracts. Arab J Chem 13(11):8248–8261. https://doi.org/10.1016/j.arabjc.2020.01.009

Clinical and Laboratory Standards Institute (CLSI). (2018) M100:Performance Standard for Antimicrobial Susceptibility Testing. 28th ed. Wayne, PA.

Clinical and Laboratory Standards Institute. (2018) M07-A11: Methods for dilution antimicrobial susceptibility tests for bacteria that grow aerobically. 11th ed. Wayne, PA.

de Souza TA, Souza LR, Franchi LP (2019) Silver nanoparticles: An integrated view of green synthesis methods, transformation in the environment, and toxicity. Ecotoxicol Environ Saf 30(171):691–700. https://doi.org/10.1016/j.ecoenv.2018.12.095

Dutta T, Chattopadhyay AP, Ghosh NN, Khatua S, Acharya K, Kundu S, Mitra D, Das M (2020) Biogenic silver nanoparticle synthesis and stabilization for apoptotic activity; insights from experimental and theoretical studies. Chem Pap 74:4089–4101. https://doi.org/10.1007/s11696-020-01216-z

Ebrahiminezhad A, Bagheri M, Taghizadeh SM, Berenjian A, Ghasemi Y (2016) Biomimetic synthesis of silver nanoparticles using microalgal secretory carbohydrates as a novel anticancer and antimicrobial. Adv Nat Sci Nanosci Nanotechnol 7(1):15018. https://doi.org/10.1088/2043-6262/7/1/015018

Feroze N, Arshad B, Younas M, Afridi MI, Saqib S, Ayaz A (2020) Fungal mediated synthesis of silver nanoparticles and evaluation of antibacterial activity. Microsc Res Tech 83:72–80. https://doi.org/10.1002/jemt.23390

Garcia AM, Bizeto MA, Ferrari VB, Okamoto DN, de Vasconcellos SP, Camilo FF (2020) Direct evaluation of microbial growth dynamics and colloidal stability of silver nanoparticles stabilized by poly (vinyl pyrrolidone) and poly (vinyl alcohol). J Nanopart Res 22:1–4. https://doi.org/10.1007/s11051-020-04863-1

Gupta N, Singh HP, Sharma RK (2011) Metal nanoparticles with high catalytic activity in degradation of methyl orange: an electron relay effect. J Mol Catal A Chem 335:248–252. https://doi.org/10.1016/j.molcata.2010.12.001

Ijaz I, Gilani E, Nazir A, Bukhari A (2020) Detail review on chemical, physical and green synthesis, classification, characterizations and applications of nanoparticles. Green Chem Lett Rev 13(3):223–245. https://doi.org/10.1080/17518253.2020.1802517

Ismail M, Gul S, Khan MI, Khan MA, Asiri AM, Khan SB (2019) Green synthesis of zerovalent copper nanoparticles for efficient reduction of toxic azo dyes congo red and methyl orange. Green Process Synth 8:135–143

Jain S, Mehata MS (2017) Medicinal plant leaf extract and pure flavonoid mediated green synthesis of silver nanoparticles and their enhanced antibacterial property. Sci Rep 7:1–3. https://doi.org/10.1038/s41598-017-15724-8

Jain A, Ahmad F, Gola D, Malik A, Chauhan N, Dey P, Tyagi PK (2020) Multi dye degradation and antibacterial potential of Papaya leaf derived silver nanoparticles. Environ Nanotechnol, Monit Manag 1(14):100337. https://doi.org/10.1016/j.enmm.2020.100337

Jiraroj D, Tungasmita S, Tungasmita DN (2014) Silver ions and silver nanoparticles in zeolite A composites for antibacterial activity. Powder Technol 264:418–422. https://doi.org/10.1016/j.powtec.2014.05.049

Keshari AK, Srivastava R, Singh P, Yadav VB, Nath G (2020) Antioxidant and antibacterial activity of silver nanoparticles synthesized by Cestrum nocturnum. J Ayurveda Integr Med 11(1):37–44. https://doi.org/10.1016/j.jaim.2017.11.003

Khan I, Saeed K, Khan I (2019) Nanoparticles: Properties, applications and toxicities. Arabian J Chem 12(7):908–931. https://doi.org/10.1016/j.arabjc.2017.05.011

Kim B, Song WC, Park SY, Park G (2021) Green Synthesis of Silver and Gold Nanoparticles via Sargassum serratifolium Extract for Catalytic Reduction of Organic Dyes. Catalysts 11(3):347. https://doi.org/10.3390/catal11030347

Kumari RM, Thapa N, Gupta N, Kumar A, Nimesh S (2016) Antibacterial and photocatalytic degradation efficacy of silver nanoparticles biosynthesized using Cordia dichotoma leaf extract. Adv Nat Sci Nanosci Nanotechnol 7(4):045009. https://doi.org/10.1088/2043-6262/7/4/045009

Lade BD, Gogle DP (2019) Nano-biopesticides: Synthesis and Applications in Plant Safety Application in Plant Protection. Springer, Cham, pp 169–189

Latif MS, Abbas S, Kormin F, Mustafa MK (2019) Green synthesis of plant-mediated metal nanoparticles The role of polyphenols. Asian J Pharmaceut Clin Res 12(7):75–84. https://doi.org/10.22159/ajpcr.2019.v12i7.33211

Lee SH, Jun BH (2019) Silver nanoparticles: synthesis and application for nanomedicine. Int J Mol Sci 20(4):865. https://doi.org/10.3390/ijms20040865

Marimuthu S, Antonisamy AJ, Malayandi S, Rajendran K, Tsai PC, Pugazhendhi A, Ponnusamy VK (2020) Silver nanoparticles in dye effluent treatment: A review on synthesis, treatment methods, mechanisms, photocatalytic degradation, toxic effects and mitigation of toxicity. J Photochem Photobiol B: Biol 2020(205):111823. https://doi.org/10.1016/j.jphotobiol.2020.111823

Mathur P, Jha S, Ramteke S, Jain NK (2018) Pharmaceutical aspects of silver nanoparticles. Artif Cells Nanomed Biotechnol 46(sup1):115–126. https://doi.org/10.1080/21691401.2017.1414825

Miean KH, Mohamed S (2001) Flavonoid (myricetin, quercetin, kaempferol, luteolin, and apigenin) content of edible tropical plants. J Agric Food Chem 49(6):3106–3112. https://doi.org/10.1021/jf000892m

Mytilinaios I, Salih M, Schofield HK, Lambert RJ (2012) Growth curve prediction from optical density data. Int J Food Microbiol 154(3):169–176

Naghili H, Tajik H, Mardani K, Rouhani SM, Ehsani A, Zare P (2013) Validation of drop plate technique for bacterial enumeration by parametric and nonparametric tests. Vet Res Forum 4(3):179

Nouri A, Yaraki MT, Lajevardi A, Rezaei Z, Ghorbanpour M, Tanzifi M (2020) Ultrasonic-assisted green synthesis of silver nanoparticles using Mentha aquatica leaf extract for enhanced antibacterial properties and catalytic activity. Colloid Interface Sci Commun 1(35):100252. https://doi.org/10.1016/j.colcom.2020.100252

Nyabola AO, Kareru PG, Madivoli ES, Wanakai SI, Maina EG (2020) Formation of silver nanoparticles via Aspilia pluriseta extracts their antimicrobial and catalytic activity. J Inorg Organomet Polym Mater. https://doi.org/10.1007/s10904-020-01497-7

Paul B, Bhuyan B, Purkayastha DD, Dhar SS (2015) Green synthesis of silver nanoparticles using dried biomass of Diplazium esculentum (retz.) sw. and studies of their photocatalytic and anticoagulative activities. J Mol Liq 212:813–817. https://doi.org/10.1016/j.molliq.2015.10.032

Prasad R, Jha AK, Prasad K (2018) Exploring the Realms of Nature for Nanosynthesis. Springer International Publishing, New York

Qais FA, Shafiq A, Khan HM, Husain FM, Khan RA, Alenazi B, Alsalme A, Ahmad I (2019) Antibacterial effect of silver nanoparticles synthesized using Murraya koenigii (L.) against multidrug-resistant pathogens. Bioinorg Chem Appl. https://doi.org/10.1155/2019/4649506

Rafique M, Sadaf I, Tahir MB, Rafique MS, Nabi G, Iqbal T, Sughra K (2019) Novel and facile synthesis of silver nanoparticles using Albizia procera leaf extract for dye degradation and antibacterial applications. Mater Sci Eng, C 1(99):1313–1324. https://doi.org/10.1016/j.msec.2019.02.059

Rajeshkumar S (2016) Synthesis of silver nanoparticles using fresh bark of Pongamia pinnata and characterization of its antibacterial activity against gram positive and gram negative pathogens. Res-Eff Tech 2(1):30–35. https://doi.org/10.1016/j.reffit.2016.06.003

Raza MA, Kanwal Z, Rauf A, Sabri AN, Riaz S, Naseem S (2016) Size-and shape-dependent antibacterial studies of silver nanoparticles synthesized by wet chemical routes. Nanomaterials 6(4):74. https://doi.org/10.3390/nano6040074

Ren YY, Yang H, Wang T, Wang C (2016) Green synthesis and antimicrobial activity of monodisperse silver nanoparticles synthesized using Ginkgo Biloba leaf extract. Phys Lett A 380(45):3773–3777. https://doi.org/10.1016/j.physleta.2016.09.029

Saad A, Snoussi Y, Abderrabba M, Chehimi MM (2016) Ligand-modified mesoporous silica SBA-15/silver hybrids for the catalyzed reduction of methylene blue. RSC Adv 6(62):57672–57682. https://doi.org/10.1039/C6RA12061J

Saeed S, Iqbal A, Ashraf MA (2020) Bacterial-mediated synthesis of silver nanoparticles and their significant effect against pathogens. Environ Sci Pollut Res 27(30):37347–37356. https://doi.org/10.1007/s11356-020-07610-0

Salim MM, Malek NA (2016) Characterization and antibacterial activity of silver exchanged regenerated NaY zeolite from surfactant-modified NaY zeolite. Mater Sci Eng C 59:70–77. https://doi.org/10.1016/j.msec.2015.09.099

Sanyasi S, Majhi RK, Kumar S, Mishra M, Ghosh A, Suar M, Satyam PV, Mohapatra H, Goswami C, Goswami L (2016) Polysaccharide-capped silver Nanoparticles inhibit biofilm formation and eliminate multi-drug-resistant bacteria by disrupting bacterial cytoskeleton with reduced cytotoxicity towards mammalian cells. Sci Rep 6(1):24929. https://doi.org/10.1038/srep24929

Shaikh S, Nazam N, Rizvi SM, Ahmad K, Baig MH, Lee EJ, Choi I (2019) Mechanistic insights into the antimicrobial actions of metallic nanoparticles and their implications for multidrug resistance. Int J Mol Sci 20(10):2468. https://doi.org/10.3390/ijms20102468

Singh P, Kim YJ, Zhang D, Yang DC (2016) Biological synthesis of nanoparticles from plants and microorganisms. Trends Biotechnol 34(7):588–599. https://doi.org/10.1016/j.tibtech.2016.02.006

Singhal A, Singhal N, Bhattacharya A, Gupta A (2017) Synthesis of silver nanoparticles (AgNPs) using Ficus retusa leaf extract for potential application as antibacterial and dye decolourising agents. Inorg Nano-Metal Chem 47(11):1520–1529. https://doi.org/10.1080/24701556.2017.1357604

Slavin YN, Asnis J, Häfeli UO, Bach H (2017) Metal nanoparticles: understanding the mechanisms behind antibacterial activity. J Nanobiotechnol 15(1):1–20. https://doi.org/10.1186/s12951-017-0308-z

Sooklert K, Wongjarupong A, Cherdchom S, Wongjarupong N, Jindatip D, Phungnoi Y, Rojanathanes R, Sereemaspun A (2019) Molecular and morphological evidence of hepatotoxicity after silver nanoparticle exposure: a systematic review, in silico, and ultrastructure investigation. Toxicolo Res 35(3):257–270. https://doi.org/10.5487/TR.2019.35.3.257

Thirumagal N, Jeyakumari AP (2020) Photocatalytic and antibacterial activities of AgNPs from Mesua Ferrea seed. SN Appl Sci 2(12):1–13. https://doi.org/10.1007/s42452-020-03650-w

Umikalsom Y, Grayer-Barkmeijer RJ, Harborne JB (1994) A comparison of the flavonoids in Athyriaceae and Aspleniaceae. Biochem Syst Ecol 22(6):587–594. https://doi.org/10.1016/0305-1978(94)90071-X

Vijilvani C, Bindhu MR, Frincy FC, AlSalhi MS, Sabitha S, Saravanakumar K, Devanesan S, Umadevi M, Aljaafreh MJ, Atif M (2020) Antimicrobial and catalytic activities of biosynthesized gold, silver and palladium nanoparticles from Solanum nigurum leaves. J Photochem Photobiol B: Biol 202:111713. https://doi.org/10.1016/j.jphotobiol.2019.111713

Wang P, Huang B, Zhang X, Qin X, Jin H, Dai Y, Wang Z, Wei J, Zhan J, Wang S, Wang J (2009) Highly efficient visible-light plasmonic photocatalyst Ag@ AgBr. Chem Eur J 15(8):1821–1824. https://doi.org/10.1002/chem.200802327

Yaqoob AA, Umar K, Ibrahim MN (2020) Silver nanoparticles: various methods of synthesis, size affecting factors and their potential applications–a review. Appl Nanosci 10(5):1369–1378. https://doi.org/10.1007/s13204-020-01318-w

Yun'an Qing LC, Li R, Liu G, Zhang Y, Tang X, Wang J, Liu H, Qin Y (2018) Potential antibacterial mechanism of silver nanoparticles and the optimization of orthopedic implants by advanced modification technologies. Int J Nanomed 13:3311–3327. https://doi.org/10.2147/IJN.S165125

Zafar S, Zafar A (2019) Biosynthesis and characterization of silver nanoparticles using Phoenix dactylifera fruits extract and their in vitro antimicrobial and cytotoxic effects. Open Biotechnol J 13(1):37–46. https://doi.org/10.2174/1874070701913010037